Work distribution of multiple Cartesian robot arms for kiwifruit harvesting

Josh Barnett, Mike Duke, Chi Kit Au, Shen Him Lim

Abstract

Employing multiple robot arms for kiwifruit harvesting can raise the efficiency since the task completion time is shortened. However, task partitioning and reachability are two major concerns. It is found that the task completion time is minimized if task partitions for robot arms are uniform. However, the partition uniformity is influenced by the fruit indivisibility and fruit cluster growing style. It is also constrained by the fruit distribution across the canopy and the robot arm positions which affect the fruit reachability. This article investigates how to partition the tasks of kiwifruit harvesting so that the harvesting can be completed by multiple robot arms in the minimum time with an assumption that the fruits can be harvested by any robot arm. A parameter termed work distribution is introduced to measure how the task partitioning is different from the optimum. A research platform with two robot arms is implemented to show how to approximate the assumption. Ten field experiments of kiwifruit harvesting had been run by the research platform in two kiwifruit orchards in New Zealand with satisfactory outcomes.

Keywords: Multiple robot arms, task partitioning, workspace, kiwifruit harvesting.

1. Introduction

The kiwifruit industry in New Zealand has been in a state of recovery in recent years after an invasive pathogen was found present in crops throughout the country during late 2010 (Everettet al., 2011). In 2018, the industry is now well recovered with annual sales revenue in excess of NZD 2 billion.

In New Zealand, up to 1.5% of the profits from kiwifruit market are allocated back into an integrated innovation program where new cultivars of kiwifruit such as the popular gold variety 'SunGold' are developed. The growth goal is to increase annual sales revenue to NZD 4.5 billion by 2025 (Zespri , 2017). To achieve this, the production volume of higher-value golden strains is planned to increase dramatically by introducing an additional 750 hectares of SunGold kiwifruit orchards per year over the next 5 years, albeit maintaining the green kiwifruit production volume.

It is forecast that by 2022, those additional SunGold orchards will have been responsible for doubling the volume of SunGold fruit from 45 million trays to over 88 million trays. As a result, the New Zealand kiwifruit industry will likely experience some challenges throughout this growth period, though one of those challenges is already prevalent today – a shortage of labour. As of May 2018, the New Zealand government has declared that the industry is short by 1200 staff with another 14000 needed by 2030.

In order to maintain the productivity of the kiwifruit industry, procedures must be taken to overcome the obstacle of labour shortage. As a result, mechanization of kiwifruit harvesting is proposed to replace jobs formerly carried out by manual labour.

2. Related Work

In 1987, an economic analysis of robotic citrus fruit harvesting in Florida found that a multiple arm harvester capable of 85% harvesting efficiency and an average harvest cycle time of three seconds would be 50% more expensive than equivalent manual labour (Harrell, 1987). It was concluded that research and development were needed to improve harvesting efficiency, harvest cycle time and harvester cost.

Following on from this, an orange harvesting system was developed in 1993 which used two, independent, electrically driven, telescopic robots - both mounted on a tracked platform vehicle (Recce, Taylor and Plebe, 1996). Both robots used cameras within the end-effectors as opposed to mounted statically on the platform. 86% of oranges were successfully located and the harvest cycle time was reported as approximately 7.5 seconds for each arm. The orange harvesting sequence for the two robot arms was determined with a neural network based on the double travelling salesman problem where the shortest possible path between all oranges was obtained.

A multiple robot arm harvesting system had been proposed for the harvesting of melons and for potential generic use (Edan, Engel and Miles, 1993). The system was essentially a rectangular frame that travels along a two-dimensional field at a constant velocity. Cartesian manipulators were mounted on the frame, each with a melon harvesting end-effector.

A multiple robot arm system for harvesting strawberry has been developed by the company Agrobot (Agrobot, 2018). Published research on this system is not widely available; however, it appears to be one of the first of its kind – a multiple robot harvesting system which may soon be ready for commercial trial. The system is claimed to be fully configurable for different strawberry row widths and consists of up to 24 robot arms.

Another system which is advertised as being close to commercial trial is the Harvest Croo strawberry harvesting robot (Harvest Croo, 2018). This robot appears to use 16 robot arms to pick strawberries in a similar fashion to the Agrobot. The system is claimed to replace more than thirty human pickers by harvesting 8 acres per day.

In New Zealand, an autonomous kiwifruit harvester was developed (Scarfe, 2012, Williams et al 2019) which would be capable of operating within variable and complex orchard environments. The system consisted of four robotic harvesting arms which were specifically designed to mimic the harvesting action of a human. Fruit location and detection were done with stereopsis, image segmentation and edge detection. The design brief for the system was to harvest four kiwifruit per second - considerably faster than harvest cycle times for other published harvesting robots at that time.

A comprehensive review in 2014 found the average, published harvesting robot was capable of harvesting 66% of produce with 5% fruit damage and a 33 second harvest cycle time. Some research has been done on the kinematic optimization of harvesting robot manipulators in order to achieve better results. The major focus remains on identification and control. Actually, employing multiple robot arm harvesting systems is a more practical approach for reducing the harvest cycle time. However, the literature a multiple robot arm harvesting systems are still limited; the challenges involved with single robot arm harvesting systems still remain very typical.

Multiple robots to complete a set of tasks have many applications (Cortés et al, 2004, Breitenmoser et al, 2010, Lee et al, 2015, Bhattacharya and Gavrilova, 2007, Sun et al, 2010) such as search and rescue, navigation, mapping etc. The workload for a robot in these applications is proportional to the area allocated to it. Voronoi tessellation is a common approach to partition the workload for each robot. One of the criteria is that each robot should have same portion of workload as others after the partitioning.

With respect to harvesting robots, multiple robot arm systems should provide an advantage over single robot arm systems by reducing the harvesting cycle time. However, the reduction is largely affected by the work done by each robot arm. In fact, the amount of kiwifruits harvested per each robot arm in a multiple robot arm system varies a lot. The variation can be large, especially when the kiwifruit distribution across the canopy is seriously non-uniform. This article presents an approach to partition the kiwifruits across the canopy and allocate them to the robot arms in a robot system so that the amount of kiwifruits harvested is approximately equal for each robot arm even though the kiwifruits are not uniformly distributed across the canopy. This can minimize the total time to harvest all the located fruits theoretically.

3. Kiwifruit harvesting

The harvesting process is performed by a robotic system with N robot arms installed on a mobile platform. At the beginning of harvesting operation, a canopy image is captured by a vision system and the three dimensional kiwifruit locations are obtained for driving the manipulator and end-effector to grab the fruits. The fruit identification and location are an off-line process. There is no additional visual sensing between successive harvesting tasks.

Most of the kiwifruit trees are grown in a rectangular array arrangement in an orchard as shown in Figure 1. The canopy is best described as a three-dimensional Cartesian system where x is the length of the orchard row, y is the width of the orchard row and z is the height variance of kiwifruit within the row.

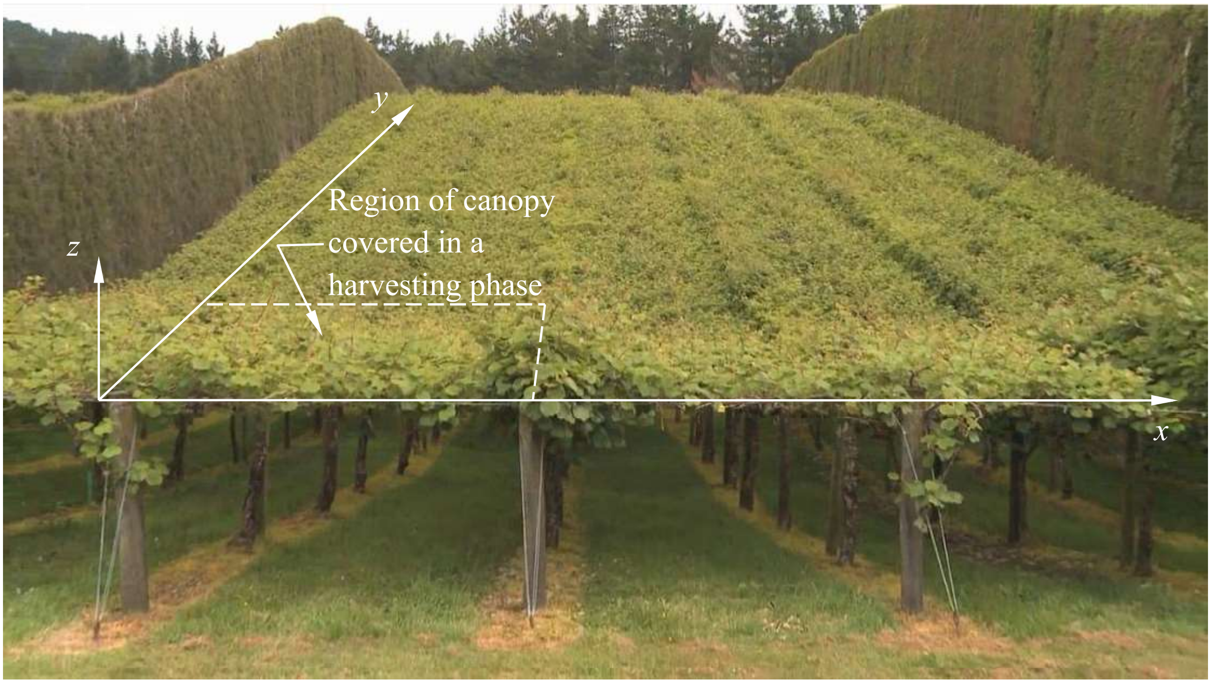

Figure 1. A kiwifruit orchard.

A harvesting phase is the process whereby the mobile platform stops, kiwifruit are detected and located, the robot arms attempt to harvest all reachable fruit, then the mobile platform advances to another region of the canopy which has not yet been harvested. A sub–phase is where the robot arm (manipulator and end–effector) will move from current location to a new fruit location and detach the fruit from the canopy. Thus, a harvesting phase is composed of n sub–phases if there are n kiwifruits located. A task refers to moving a robot arm from its current position and harvesting a kiwifruit at locations $\boldsymbol{p}_i$ ($i \in [1,n]$) in the task space $\boldsymbol{S_T}$.

Due to the coordinate system of the canopy, a set $\boldsymbol{R}$ of N robot arms ($\boldsymbol{r}_j$, $j \in [1,N]$) should be positioned sequentially along the x axis of the canopy to harvest the kiwifruits.

A scheduler is a software implementation to schedule the kiwifruit harvesting. It reads the kiwifruit locations from the vision system, partitions the locations into N sub-spaces $\boldsymbol{S}_j$ ($j \in [1,N]$, $\boldsymbol{S}_T = \cup_j \boldsymbol{S}_j$) so that an allocation function $A{:}\boldsymbol{S}_T \rightarrow \boldsymbol{R}$ is established. It also determines the fruit harvesting order within the sub-space $\boldsymbol{S}_j$ so that each set of fruits is harvested by the corresponding robot arm $\boldsymbol{r}_j$ (i.e. such that $\boldsymbol{r}_j = A(\boldsymbol{S}_j)$).

Problem formulation: How should the task space $\boldsymbol{S}_T$ be partitioned into N partitions ($\cup_j \boldsymbol{S}_j = \boldsymbol{S}_T$) so that they can be completed by the robot arms ($\boldsymbol{r}_j \in \boldsymbol{R}$, $j \in [1,N]$) with the minimum time?

4. Work distribution

Let $n_1, n_2, \ldots, n_N$ be the number of tasks (kiwifruit locations) in each sub–spaces $\boldsymbol{S}_j$ ($j \in [1,N]$) and assume that a task $\boldsymbol{p}_i$ ($\forall i \in [1,n]$) can be completed by any robot arm $\boldsymbol{r}_j$ ($\forall j \in [1,N]$).

Definition 1: Work load L_j performed by a robot arm $\boldsymbol{r}_j$ is defined as a ratio of the number of tasks n_j completed by a robot arm to the total number of tasks n

$$L_i = \frac{n_j}{n} \tag{1}$$

Lemma 1: If the maximum workload of the robot arm is L_{max} (such that $L_{max} \leq 1$), then

$$L_{max} \geq \frac{1}{N} \tag{2}$$

Proof: Let L_{max} be the maximum workload and L_{max}, L_2, ..., L_N be the workload of the N robot arms so that $L_{max} + \sum_{j=2}^{N} L_j = 1$. Assume that $L_{max} < \frac{1}{N}$, then $L_j < L_{max} < \frac{1}{N}$. Hence $L_{max} + \sum_{j=2}^{N} L_i < N \cdot \left(\frac{1}{N}\right)$ or $L + \sum_{j=2}^{N} L_j < 1$. This contradicts with $L + \sum_{j=2}^{N} L_j = 1$. Hence the assumption of $L_{max} < \frac{1}{N}$ is false and $L_{max} \geq \frac{1}{N}$. □

Lemma 2: If the maximum workload of a robot arm is L_{max} (such that $L_{max} \leq 1$), then the equivalent number of robot arms performing the maximum workload L_{max} to complete all the tasks is $\frac{1}{L_{max}}$.

Proof: Since the maximum workload perform by the busiest robot arm is L_{max}, then the rest of the workload $1 - L_{max}$ should be performed by the rest of $N - 1$ robot arms. Let n' be the equivalent number of robot arms performing maximum workload L_{max} to complete the workload of $1 - L_{max}$ so that $n' \cdot L_{max} = 1 - L_{max}$ which implies $n' = \frac{1 - L_{max}}{L_{max}}$. Hence the total number of robot arms performing maximum workload of L_{max} to complete all the tasks is $n' + 1 = \frac{1}{L_{max}}$. $\square$

Definition 2: Work distribution W_D is defined as a unitless ratio of the average theoretical workload $\frac{1}{N}$ at parity to the maximum workload L_{max} performed by a robot arm in a multiple robot arm system. Hence

$$W_D = \frac{1}{N \cdot L_{max}} \tag{3}$$

Lemma 3: The maximum value of work distribution W_D is one.

Proof: From Lemma 1, $L_{max} \geq \frac{1}{N}$ which implies $W_D = \frac{1}{L_{max} \cdot N} \leq 1$. Hence, the maximum value of W_D is 1. $\square$

Corollary 3: The workload is uniformly distributed among N robot arms if and only if $W_D = 1$.

Proof: Since the workload is uniformly distributed among N robot arms, then the maximum workload $L_{max} = \frac{1}{N}$ which implies $\frac{1}{L_{max} \cdot N} = 1$. Hence, from the definition of work distribution, $W_D = 1$.

When $W_D = 1$, from the definition of work distribution $\frac{1}{N \cdot L_{max}} = 1$. Hence, $L_{max} = \frac{1}{N}$ which implies the workload is uniformly distributed among N robot arms. $\square$

Introducing the total time t_{total} to complete all the tasks in task space $\boldsymbol{S}_T$,

$$t_{total} = \max\,(n_1 \cdot t_s, \ldots, n_N \cdot t_s)$$

where t_s is the sub-phase time for the robot arm to reach from one location to another location.

Lemma 4: The time to complete the all tasks t_{total} is expressed as

$$t_{total} = \frac{n \cdot t_s}{N \cdot W_D} \tag{4}$$

Proof: The time for the multiple robot system with N to complete a task of visiting n points is $t_{total} = \max(n_1 \cdot t_s, ..., n_N \cdot t_s)$. Rewriting $t_{total} = \max\left(\frac{n_1}{n} \cdot t_s, ..., \frac{n_N}{n} \cdot t_s\right) \cdot n$ which is equivalent to $t_{total} = \max(L_1 \cdot t_s, ..., L_{max} \cdot t_s) \cdot n$ or $t_{total} = L_{max} \cdot t_s \cdot n$. From definition 2, $t_{total} = \frac{n \cdot t_s}{N \cdot W_D}$ □

Hence, the optimal partitioning approach to complete the task is obtained with work distribution $W_D = 1$, which means allocating the number of tasks to each robot arm uniformly. This yields the minimum time to complete all the tasks. However, the tasks may not be divisible. Each task must be allocated entirely to a single robot arm.

A sub-optimal partitioning approach is employed if the number of tasks n is not divisible by the number of robot arm N. The tasks are partitioned such that $N - r$ partitions consist of $\frac{n-r}{N}$ tasks and r partitions have $\frac{n-r}{N} + 1$ tasks, where $r = n \bmod N$ and $r \neq 0$).

Lemma 5: The work distribution with the sub-optimal partitioning approach is bounded by $\frac{n}{N+n}$ and 1.

Proof: Partitioning n task points into N partitions yields $N - r$ partitions of $\frac{n-r}{N}$ task points and r partitions of $\frac{n-r}{N} + 1$ task points where $0 \leq r \leq N$. Hence, the average theoretical workload is $\frac{n}{N}$ and the maximum workload is $\frac{n-r}{N} + 1$. This gives $W_D = \frac{n}{n-r+N}$. Since $0 < r < N$ which implies $\frac{n}{N+n} < \frac{n}{n-r+N} < 1$.

As a result, $\frac{n}{n+N} < W_D < 1$. □

Corollary 5: The sub-optimal partitioning approach yields a work distribution of 1 when the number of tasks in each set $\boldsymbol{S}_j$ is large.

Proof: Since $\frac{n}{n+N} < W_D < 1$, $\lim_{n \to \infty} \frac{n}{n+N} < \lim_{n \to \infty} W_D < 1$. Hence $\lim_{n \to \infty} W_D = 1$ as $N \ll n$. □

Hence, a task space $\boldsymbol{S}_T$ (with n tasks) should be partitioned into $N - r$ sub–spaces with $\frac{n-r}{N}$ tasks and r sub–spaces with $\frac{n-r}{N} + 1$ tasks (where $r = n \bmod N$) in order to complete all tasks by N robot arms in the minimum time with the assumption that a task $\boldsymbol{p}_i$ ($\forall i \in [1,n]$) can be completed by any robot arm $\boldsymbol{r}_j$ ($\forall j \in [1,N]$).

5. Implementation

The conditions for obtaining the minimum time to complete all the tasks consist of two parts: assumption and task partition. These two parts are implemented to build a multiple robot arm system for kiwifruit harvesting. In the harvesting process, a kiwifruit location in the canopy represents a task which includes robot arm movement from its current position and harvesting. A harvesting task is defined as:

i. Moving the end-effector from its current position to the target fruit position and
ii. Harvesting the target fruit (the harvested fruit drops into the container due to gravity).

5.1 Assumption approximation

A task $\boldsymbol{p}_i$ ($i \in [1,n]$) can be completed by a robot arm $\boldsymbol{r}_j$ ($j \in [1,N]$) if and only if the task locates inside the work space $\boldsymbol{W}_S^j$ of robot arm (i.e. $\boldsymbol{p}_i \in \boldsymbol{W}_S^j$). For a multiple robot arm system, the assumption of a task can be completed by any robot arm is not practical since it means the resultant workspace $\boldsymbol{W}_S$ of all the robot arm workspace $\boldsymbol{W}_S^j$ equal to the intersection of all robot arm workspaces $\cap_j \boldsymbol{W}_S^j$ (i.e. $\boldsymbol{W}_S = \cup_j \boldsymbol{W}_S^j = \cap_j \boldsymbol{W}_S^j$). However, as the robot arms are arranged sequentially along the *x* axis of the canopy, the assumption can be approximated by having a large common work space $\boldsymbol{W}_S^j \cap \boldsymbol{W}_S^{j+1}$ between two consecutive robot arms $\boldsymbol{r}_j$ and $\boldsymbol{r}_{j+1}$ ($j \in [1,N-1]$).

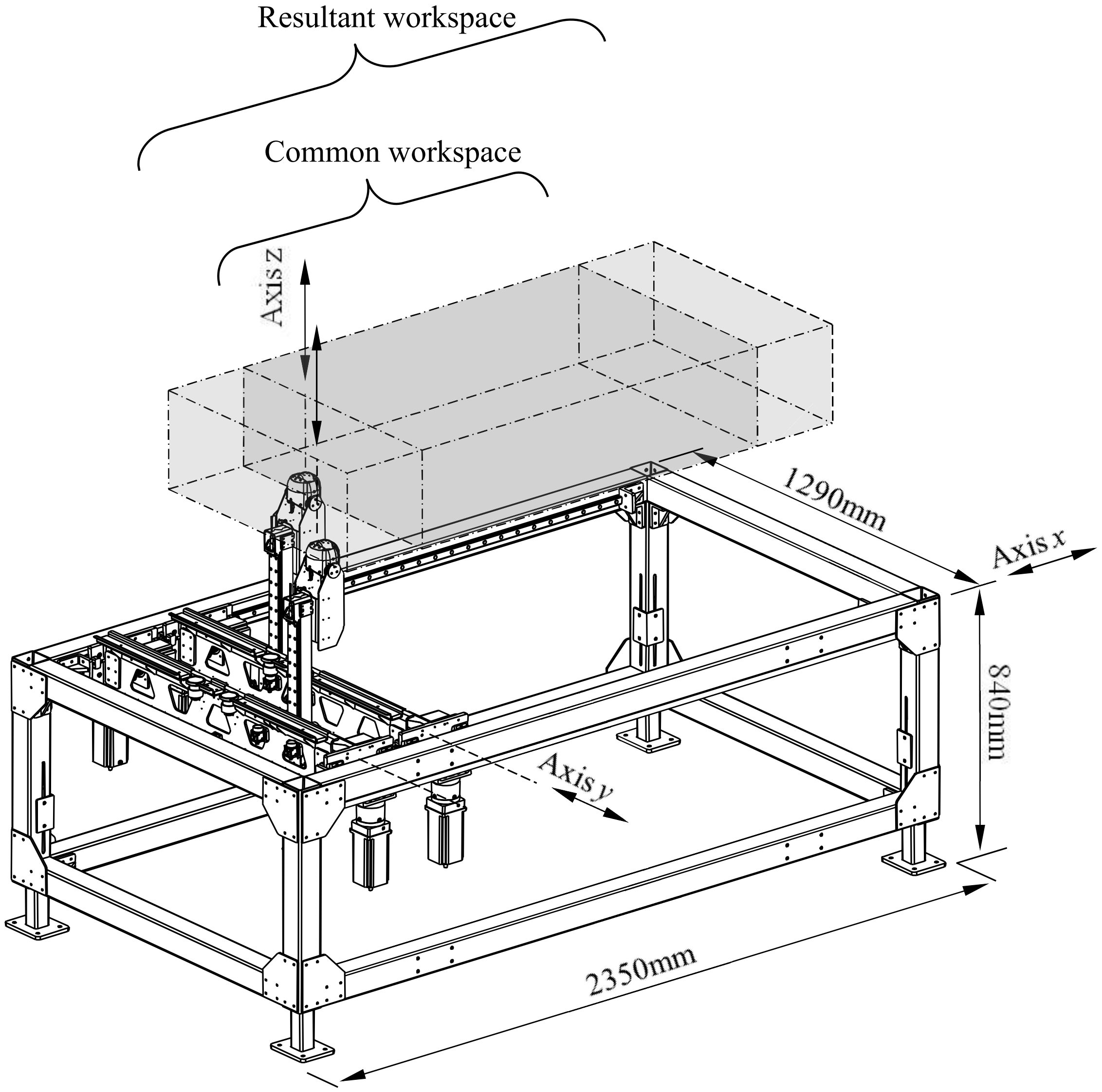

Figure 2. A kiwifruit harvesting robot with two robot arms.

A prismatic axis, linear rail constrained, kiwifruit harvesting robot with two robot arms is developed as a research platform to investigate the work distribution among the robot arms in a multiple robot system for kiwifruit harvesting. The overall dimension of the robotic system is 840mm×1290mm×2350mm. It is a two–robot arm, prismatic axis kiwifruit harvesting robot. This prismatic axis system is Cartesian where each robot arm has an x, y and z axis as depicted in Figure 2. The x axis on each robot will be common such that the robot-arms can move synchronously throughout a shared workspace. Each axis will be comprised of a linear rail system for motion constraint as shown. This robot arm is of three degrees of freedom. The limits for axis x, y and z are 1500mm, 650mm and 450mm which yields a rectangular workspace volume. The workspace is coloured grey in the Figure. The region with deep grey indicates common workspace. Figure 3 shows the multiple robot system in the orchard.

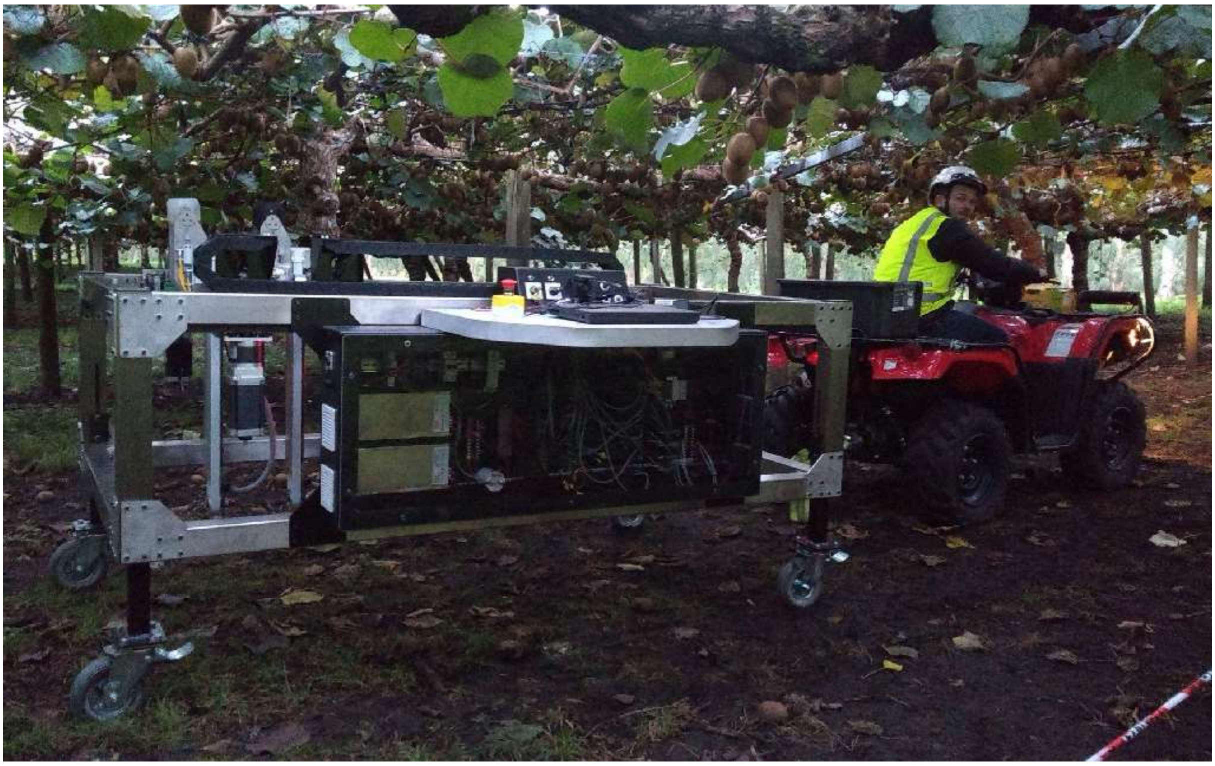

Figure 3. The multiple robotic system in the kiwifruit orchard.

5.2 Task partitioning

The task partitioning is implemented in a scheduler by defining a *key* operator and a *sort* operator so that the optimal (or sub-optimal) partitioning is achieved.

Definition 3: A *key* function K is defined from the task space $\boldsymbol{S}_T$ to a key space $\boldsymbol{S}_K$, K:$\boldsymbol{S}_T$→ $\boldsymbol{S}_K$ such that $x_i = \mathrm{K}(\boldsymbol{p}_i)\ \forall \boldsymbol{p}_i = [x_i \quad y_i \quad z_i]^T \in \boldsymbol{S}_T$ and $x_i \in \boldsymbol{S}_K$.

Definition 4: A *sort* operator Σ is defined to sort the elements of a set, Σ:$\boldsymbol{S}_K$→$\boldsymbol{S}^{sorted}_K$ such that $\boldsymbol{S}^{sorted}_K = \Sigma(\boldsymbol{S}_K) = \{x_i | x_{i-1} < x_i\ \forall x_i \in \boldsymbol{R},\ i = 1,2,...,n\}$

The tasks should be partitioned into N sub–spaces $\boldsymbol{S}_j$ ($j \in [1,N]$) along the *x* axis so that these tasks can be completed by the corresponding robot arm $\boldsymbol{r}_j$. The *x* coordinates of the tasks are extracted as the key for sorting for partition.

A sorted key space $\boldsymbol{S}^{sorted}_K = \{x_1, x_2,...,x_n | x_1 < x_2 < ... < x_n\}$ is established based on n points in the task space by applying the sort operator Σ on the key space $\boldsymbol{S}_K$ obtained from the key operator K. Based on the sorted key space, a list of points $\boldsymbol{q}_i \in \boldsymbol{S}_T$ (i = 1, 2, …,n) is sorted.

This list of sorted points is partitioned according to the number of robot arms N such that $N - r$ (where $r = n\ mod\ N$ and $r \neq 0$) partitions consist of $\frac{n-r}{N}$ points and r partitions have $\frac{n-r}{N} + 1$ points.

Once the fruit coordinates are obtained from the vision system, their *x* coordinates are extracted by the *key* operator and are sorted into *N* partitions by the *sort* operator such that each partition is allocated to a robot arm. The fruits with in a partition are preliminarily scheduled to be harvested according to the ascending order of their *x* coordinates. The allocated work distribution W_D is expressed as

$$W_D = \frac{\bar{n}}{n_{max}} \tag{5}$$

where $\bar{n}$ is the average theoretical number of fruits to be harvested by each robot arm;
n_{max} is maximum number of fruits to be harvested by a robot arm.

Moreover, instead of being uniformly spaced, kiwifruit typically grow in clusters. The kiwifruits grown within a cluster are described as having dependencies when there are fruits underneath. This may affect the harvesting performance as the end-effector may knock off the dependent fruits when it harvests a target fruit. Since the end-effector approaches the kiwifruits from the bottom, those fruits without dependencies must be harvested prior to the others. As a result, the fruits within a cluster allocated to two different robot arms may need to be re-allocated and re-scheduled so that the cluster is harvested by one robot arm.

For instance, Figure 4 illustrates the situation of fruit re-allocation and re-scheduling. Figure 4(a) shows two sets of $\bar{n}$ fruits $n_1^j, \cdots, n_{\bar{n}}^j$ (white fruits) and $n_1^{j+1}, \cdots, n_{\bar{n}}^{j+1}$ (grey fruits) allocated to two robots $\boldsymbol{r}_j$ and $\boldsymbol{r}_{j+1}$ respectively. These fruits are scheduled to be harvested according to their *x* coordinates established on the robot frame. The harvesting orders are listed by the subscripts from 1 to $\bar{n}$. Both top view and front view are included in the figure to show the relative positions of fruits. Fruit n_1^j and n_1^{j+1} will be the first fruit to be harvested by the robot arms. However, fruit $n_{\bar{n}-2}^j$, $n_{\bar{n}-1}^j$,$n_{\bar{n}}^j$,$n_1^{j+1}$and n_2^{j+1} are in a cluster and fruit $n_{\bar{n}-2}^j$, $n_{\bar{n}-1}^j$and $n_{\bar{n}}^j$ are below fruit n_1^{j+1}, they are dependencies to fruit n_1^{j+1}. As the end-effector of robot $\boldsymbol{r}_{j+1}$ approaches the fruit n_1^{j+1} from the bottom, fruit $n_{\bar{n}-2}^j$, $n_{\bar{n}-1}^j$and $n_{\bar{n}}^j$ may be knocked off. Hence, the dependent fruit $n_{\bar{n}-2}^j$, $n_{\bar{n}-1}^j$and $n_{\bar{n}}^j$ have to be re-allocated to robot $\boldsymbol{r}_{j+1}$and re-scheduled for harvesting. Those fruits without dependency will be prioritized to be harvested as shown in Figure 4(b). Hence, when a scheduled fruit allocated to a robot arm $\boldsymbol{r}_{j+1}$ has dependencies (which are allocated to the robot arm $\boldsymbol{r}_j$), all dependencies (and potentially sub-dependencies) will be reallocated to robot arm $\boldsymbol{r}_{j+1}$. Therefore, a robot arm may lose its fruits, which are dependencies, to another robot arm. Among these re-allocated fruits, the one without dependency will be scheduled first. When a fruit has all its dependencies scheduled, it is considered as no dependency and will be scheduled (details of the fruit scheduling can be found in reference (Barnett, 2018)). Hence, the optimal or sub-optimal partitioning approach is influenced because of the harvesting order due to the cluster growing style.

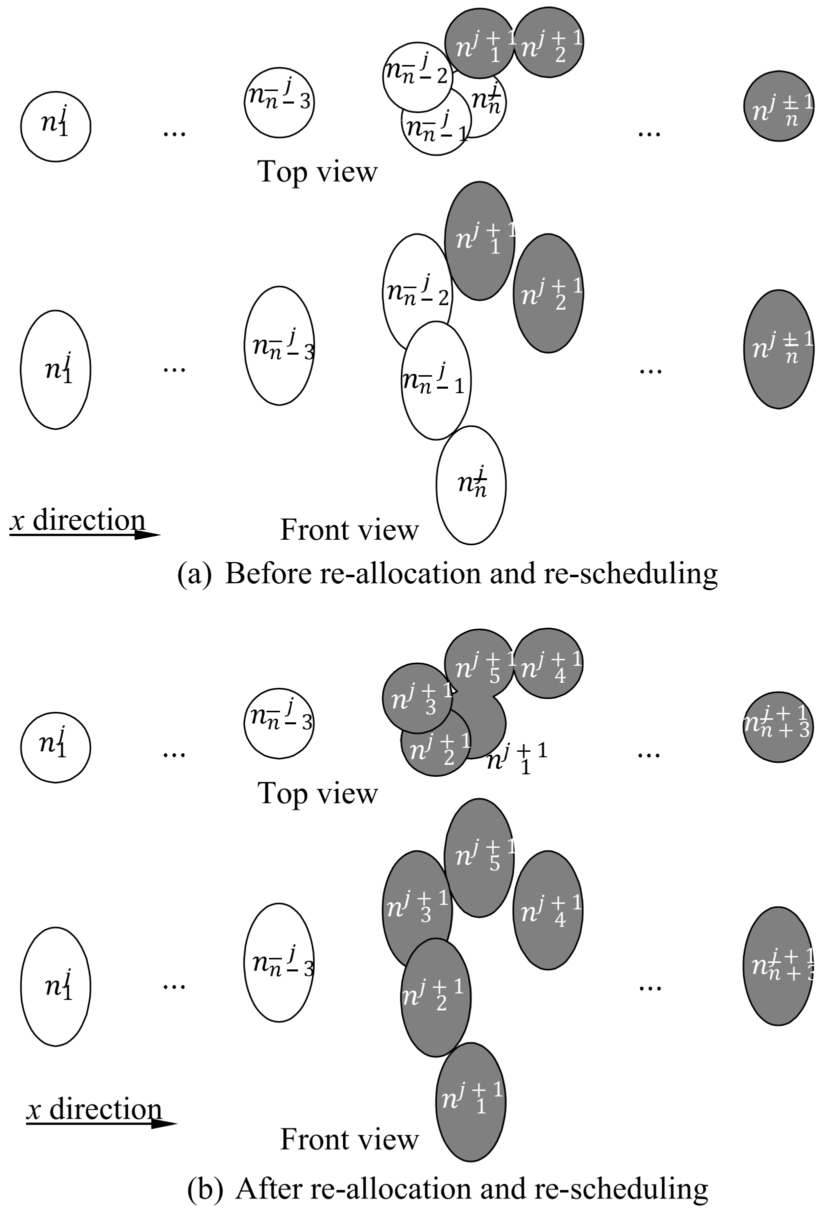

Figure 4. Fruit re-allocation and re-scheduling.

6. Field experiment

The field test aim is to investigate how the work distribution W_D among the robot arms according to the lemmas and corollaries developed for a multiple-robot system to perform kiwifruit harvesting. The kiwifruit harvesting performance was evaluated over 10 phases of static workspace; five from the Batemans orchard and five from the Newnham orchard. Both orchards grow Hayward strain kiwifruit with a pergola style located in Tauranga, New Zealand. Figure 5 shows the harvesting using the two robot arm system in the orchard.

Figure 5. Harvesting the kiwifruits using the two robot arm system.

At each region, the total number of reachable fruits located by the vision system was obtained. The average theoretical workload is calculated by dividing this number of reachable fruits by the number of robot arms. The allocated work distribution W_D was measured using definition 1 as a ratio of the workload by each robot-arm at parity to the maximum workload by a robot arm. In the kiwifruit harvesting application, it is a ratio of the average number of kiwifruits per robot arm to the maximum number of fruits allocated to the robot arm. Through the scheduler, the fruits were allocated to each robot arm. The actual work distribution W_D was obtained by using the maximum workload by a robot after re-allocation and re-scheduling. The values are shown in Table 1.

Table 1. Work distribution W_D across 10 recorded regions of kiwifruit orchard canopy.

Orchard region	Work distribution W_D	
	Actual value	Allocated value
1	1	1
2	0.98	0.98
3	0.93	1
4	0.88	0.97
5	0.94	0.98
6	0.93	1
7	0.97	0.97
8	0.94	1
9	0.84	1
10	0.97	0.97

The mean average W_D value is 0.94 across all regions. This means that the maximum workload by the most loaded robot arm is, on average, within 6% of an ideal parity work distribution. Limitations to achieving parity ($W_D = 1$) are due to the total number of fruit not perfectly divisible by the number of robot arms, but of more significance is the effect of fruit dependencies.

7. Discussion

The work distribution W_D depends on the task partitioning which is implemented in the scheduler. In fact, the workload allocated to a robot arm is expressed in terms of a task partition. A good partitioning strategy can yield the maximum work distribution of one ($W_D = 1$). Since factory automation usually provides a static and structural environment for robot applications; most of the tasks allocated to a specific robot arm are reachable and the tasks are completed. Therefore, the work distribution for a multiple robot arm system is well controlled in manufacturing. However, some applications such as agricultural robotics, certain tasks have to be transferred from one task partition to another partition due to the unstructured tasks and dynamic environment. For instance, the cluster growing style in kiwifruit growth causes the transfers of fruits from a partition to its neighbour partition. As a result, the actual work distribution deviates from the optimal value and sometimes this deviation can be large. In fact, the work distribution W_D is a measure of how close the task partition is to the optimal. This can be used as a system performance index for two robotic systems, both mechanical design and scheduler implementation.

If the workload distributed uniformly among N robot arms, then the total time to complete all the tasks is $\frac{n \cdot t_s}{N}$. From Lemma 4, the total time to complete all the tasks is $\frac{n \cdot t_s}{N \cdot W_D}$ if the workload is non-uniformly distributed among the robot arms. Comparing these two expressions shows that N robot arms with non-uniform workload distribution is equivalent to $N \cdot W_D$ ($W_D < 1$) robot arms with maximum workload among the non-uniform workload distribution. Obviously, the total time to complete all the tasks will be shorter for uniform workload distribution.

Uniform task partitioning and allocation to achieve the minimum total time for completing all the tasks are based on the assumption that a task can be completed by the allocated robot arm. The research platform has a *configuration* of common *x* axis for both robot arms. The platform is positioned in the orchard with this *x* axis aligned with the length of the orchard row so that it conforms to the structured, less variable kiwifruit orchard architecture. This assumption is approximated by have a large common workspace between two neighbouring robot arms in kiwifruit harvesting.

In fact, this approximation can be extended to a robot system with more than two arms. Figure 6 depicts the workspace of a kiwifruit harvesting robot with four arms which consists of seven partitions. The central partition (partition 4) is a common partition for all four robot arms. As a result, a task in this partition can be completed by any of these four robot arms. Furthermore, the tasks in any other partitions can be completed by at least two robot arms except those in the first (partition 1) and last partition (partition 7). These two partitions are small in size compared with the whole workspace. As a result, the assumption that a task in the workspace can be completed by any of the robot arms is well approximated.

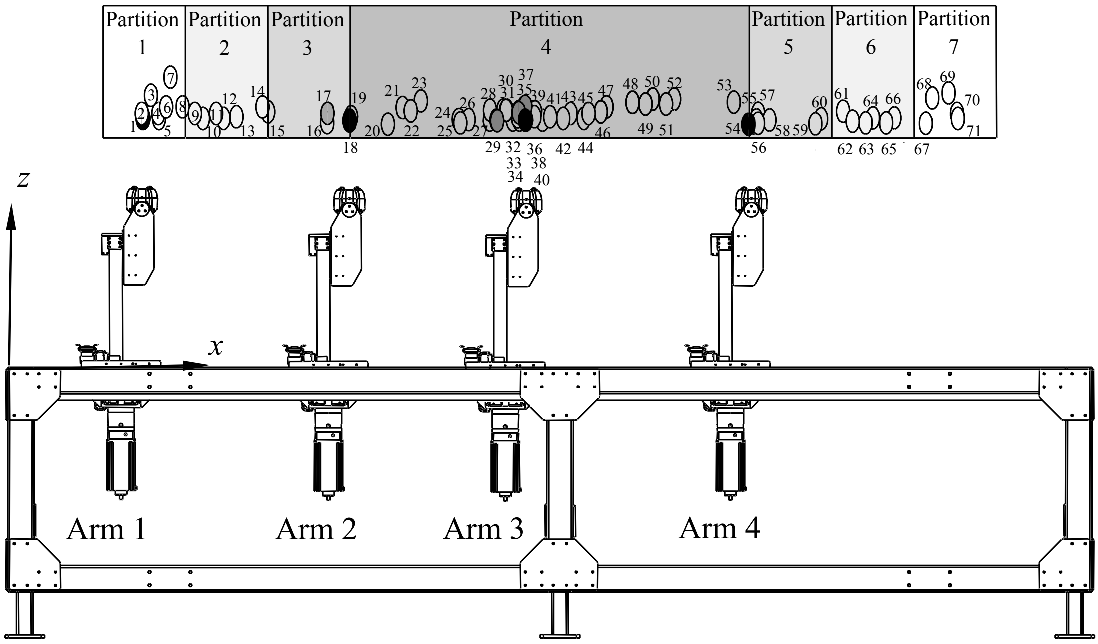

Figure 6. The workspace of a kiwifruit harvesting robot with four robot arms

However, a large common workspace implies a high risk of collision when the robot arms are operated within this common region. Since the scheduler sorts the fruits according to the *x* coordinates of their locations, partitions and allocates them to the robot arms, the robot arms start harvesting according to the sorted order of the fruits. In the example shown in Figure 6, there are totally 71 fruits hang on the canopy. The fruits are numbered according to their *x* coordinates from the coordinate system established on the robot frame. These fruits are allocated as following: fruit 1 to fruit 17 (17 fruits) are allocated to arm 1, fruit 18 to 35 (18 fruits) are allocated to arm 2, fruit 36 to 53 (18 fruits) are allocated to arm 3 and fruit 54 to 71 (18 fruits) are allocated to arm 4. The harvesting starts from the smallest numbered fruit by each arm. Hence, arm 1, 2, 3 and 4 start at the positions under the fruit 1, 18, 36 and 54 (these fruits are coloured back in the figure) respectively and harvest according to the numerical order of the fruits. Hence, all robot arms are generally travelling in the same *x* axis direction (from the left to the right) and will consistently finish their tasks at the same side of their workspace. Because of this special design of *configuration*, robot arm collision is avoided.

Since the work distribution is determined by the task partitioning for a multiple robot system, it is closely related with the configuration of the robot arm and the robot arm arrangement as these two factors determine the resultant workspace and the *common workspace* among the robot arms. A common approach of partitioning is based on the shortest distance between the robot arm and the fruits. A task at position $\boldsymbol{q}_i \in \boldsymbol{S}_W$ is completed by a robot arm at $\boldsymbol{r}_j$ ($j = 1, 2, \ldots, N$) if

$$|\boldsymbol{q}_i - \boldsymbol{r}_j| < |\boldsymbol{q}_i - \boldsymbol{r}_k|, \forall j, k \in [1, \ldots, N] \wedge j \neq k \tag{5}$$

This task partitioning is equivalent to partition the resultant workspace $\boldsymbol{S}_W$ according to Voronoi partition. Since the workspace is partitioned by a clearly defined boundary, the robot arm collision can be avoided. The work distribution can be close to one if the tasks are uniformly distribution across the resultant workspace. However, in some cases, the task distribution can be relatively non-uniform. The work distribution can be far from one due to the non-uniform task distribution.

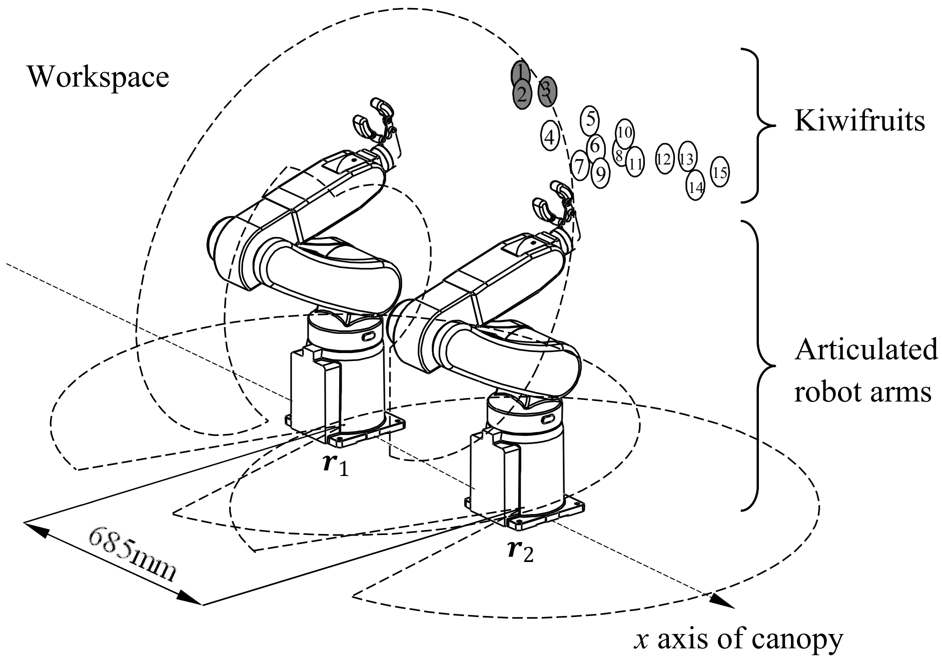

(a) Two articulated robot arms

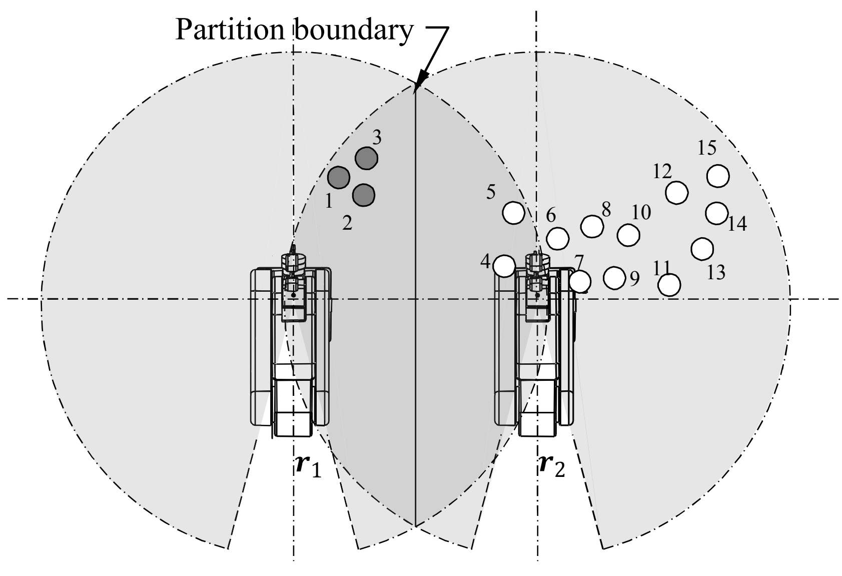

(b) Task partitioning

Figure 7. Task partitioning based on the shortest distance.

Figure 7 and 8 show an example to illustrate the difference between work distributions due to task partitioning based on the shortest distance and sorted kiwifruit position. For instance, two articulated robot arms (Hiwin, RA605) $\boldsymbol{r}_1$ and $\boldsymbol{r}_2$ arranged along the canopy x axis are employed for kiwifruit harvesting as shown in Figure 7. Figure 7(a) depicts the workspace geometries of the robot arms. Since the bases of the robot arms are fixed, the common workspace between two robot arms is relatively small. Therefore, the assumption for task partitioning based on the sorted tasks along the *x* coordinates is not fulfilled. The task partitioning has to be based on the shortest distance between the fruit and the robot arm.

Suppose there are fifteen kiwifruits non-uniformly distributed in the resultant workspace and are harvested by these two robot arms. The resultant workspace is evenly partitioned based on the closest distance between the fruit and robot arm. As a result, three kiwifruits (fruit 1 to 3) are allocated to robot arm $\boldsymbol{r}_1$ and twelve kiwifruits (fruit 4 to 15) are allocated to robot arm $\boldsymbol{r}_2$ as illustrated in Figure 7(b). The work distribution will be $\frac{7.5}{12} = 0.625$.

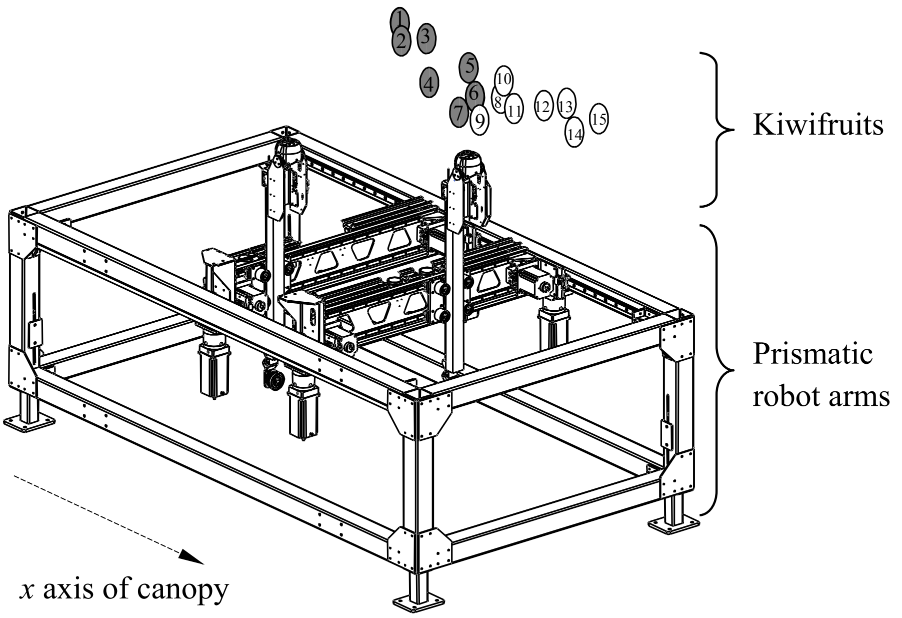

(a) A two robot system

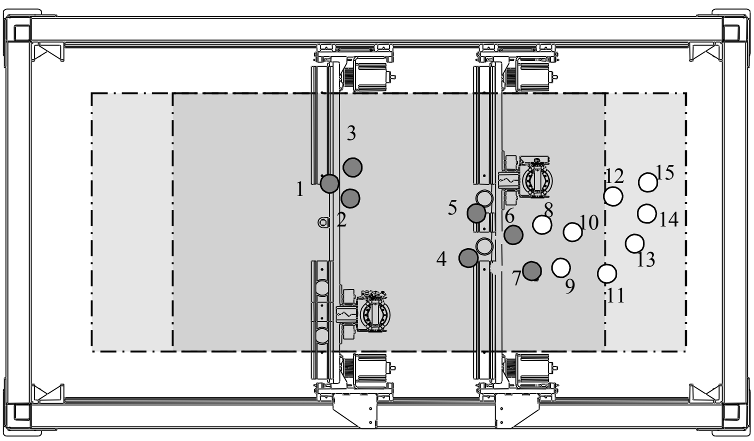

(b) Task partitioning

Figure 8. Task partitioning based on kiwifruit position.

The work distribution of harvesting fifteen kiwifruits using the research platform (a two robot system with prismatic axes) is shown in Figure 8(a), work distribution based on sorted kiwifruit position approach allocates the first seven fruits to the first robot arm and the rest of eight fruits to the second robot arm as illustrated in Figure 8(b). Hence, the work distribution is $\frac{7.5}{8} = 0.9375$ which is larger than 0.625. Furthermore, robot arm 1 and 2 start harvesting fruit 1 and 8 respectively and the harvesting order follows the numerical order according to their x coordinates. Hence, the robot arm collision can be avoided.

This example shows how the non-uniform task distribution across the workspace influences the work distribution among the robot arms and how the sorted kiwifruit position dilutes the effect of fruit distribution non-uniformity.

Table 2 lists the work distribution W_D for two articulated robot system and two Cartesian robot system. The major difference between these two systems is their *common workspaces*. The two Cartesian robot system has a common workspace shared by both arms while the two articulated robot system does not have any workspace common to both robot arms Hence, the assumption that a task can be completed by any robot arm is better approximated in the Cartesian robot system. This can be shown by the higher work distribution in the Cartesian robot system. The calculated time t_{total} to complete the harvesting of n fruits (after the fruit identification and location) based on the sub-phase time of 2s (which is obtained statistically) according equation (4) is also tabulated. The times t_{total} for Cartesian robot to complete the tasks are shorter than that of the articulated robot system as its work distributions are closer to one.

Table 2. Mean average work distribution W_D (after the fruit re-allocation and re-scheduling) across 10 recorded regions of kiwifruit orchard canopy.

Orchard region	Number of fruits n	Two Cartesian robot system		Two articulated robot system	
		W_D	t_{total}(s)	W_D	t_{total}(s)
1	62	1	62.00	0.93	66.66
2	51	0.98	52.04	0.93	54.84
3	28	0.93	30.10	0.53	52.82
4	35	0.88	39.78	0.5	70.00
5	47	0.94	50.00	0.66	71.22
6	26	0.93	27.96	0.51	50.98
7	31	0.97	31.96	0.6	51.66
8	34	0.94	36.18	0.54	62.96
9	52	0.84	61.90	0.86	60.46
10	35	0.97	36.08	0.48	72.92

Fruit identification and location are one of the key factors affecting the performance of harvesting robot. Table 3 lists the percentage of fruit harvested, dropped and missed across 10 regions of orchard taskspace by the two Cartesian robot system. It can be seen that some regions have relatively large dropped and missed percentage than the others depending on the fruit growing conditions.

Table 3. Kiwifruit harvesting performance across 10 regions.

Orchard region	Harvested (%)	Dropped (%)	Missed (%)
1	81	16	2
2	80	0	20
3	93	7	0
4	57	14	29
5	72	15	13
6	54	19	27
7	87	13	0
8	76	18	7
9	81	8	11
10	86	11	3

The dropped fruits are mainly knocked off by the end-effector. This usually happens when some fruits grow closely in a cluster and ripen earlier than the others. Small percentage of fruits is missed because of the false positions of scheduled fruits. Since the vision system captures the canopy image at the beginning of the harvesting task and fruits are located. This is an off-line process and no modification for fruit location can be made once the harvesting task starts. However, the fruits in a cluster are usually closely packed. As some of the fruits within a cluster are harvested, the positions others may shift and cause positional errors. Currently, the missed fruits are manually picked. A real time fruit identification and location may solve this issue. However, the robustness of the system is the major obstacle.

8. Conclusion

Employing multiple robot arms to perform a set of tasks can decrease the total completion time. It is shown that the minimum completion time can be achieved by uniformly partitioning and distributing the tasks among multiple robot arms with the assumption that a task can be completed by any robot arm.

In kiwifruit harvesting application, the multiple robot arms are arranged sequentially due to the architecture of orchard. A research platform is implemented to show how the assumption is approximated. A fruit harvesting scheduler is also proposed which sorts the fruits along the robot arm arrangement direction and partition them to yield the optimal (or sub-optimal) task completion time. However, the task partition deviations arise due to the indivisible fruit and fruit cluster growing style. These deviations can be measured by a parameter of work distribution which is a ratio of uniform workload performed by each robot arm to the maximum workload performed by the busiest robot arm. The difference in work distribution between the proposed task partitioning approach and the common Voronoi partitioning due to non-uniform fruit distribution is illustrated by an example.

The efficiency of kiwifruit harvesting using multiple robot arms is determined by both the configuration of the robot system and the scheduler. The robot system configuration approximates the assumption while the scheduler partitions the tasks.

Acknowledgement

This research was supported by the New Zealand Ministry for Business, Innovation and Employment (MBIE).

References

[1] Everett, K.R., Taylor, R.K., Romberg, M.K., Rees-George, J., Fullerton, R.A., Vanneste, J.L., Manning, M. A., 2011. First report of Pseudomonas syringae pv. actinidiae causing kiwifruit bacterial canker in New Zealand," Australasian Plant Disease Notes 6, 67-71.
[2] Zespri 2017. 5 YEAR OUTLOOK, technical report.
[3] Harrell, R. 1987. Economic Analysis of Robotic Citrus Harvesting in Florida, Transactions of the ASAE 30(2) 298-304.
[4] Recce,M., Taylor, J., Plebe, A., Tropiano, G., 1996. Vision and neural control for an orange harvesting robot, Proceedings of International Workshop on Neural Networks for Identification, Control, Robotics and Signal/Image Processing **DOI:** 10.1109/NICRSP.1996.542791
[5] Edan, Y., Engel, B. A., Miles, G. E., 1993. Intelligent control system simulation of an agricultural robot, Journal of Intelligent & Robotic Systems 8, 267-284.
[6] AGROBOT - Strawberries Harvester. http://agrobot.com, 2018 (accessed 6 June 2019).
[7] Harvest Croo, http://www.harvestcroorobotics.com, 2018 (accessed 6 June 2019).
[8] Scarfe, A.J., 20102. Development of an autonomous kiwifruit harvester. PhD thesis, Massey University.
[9] Williams, H., Jones, M.H., Nejati, M., Bell, J., Penhall, N., Seok, H.A., Lim, J., MacDonald, B., Seabright, M., Barnett, J., Duke, M., Scarfe, A. 2019. Robotic Kiwifruit Harvesting using Machine Vision, Convolutional Neural Networks, and Robotic Arms, Biosystems Engineering 181, 140-156.
[10] Cortés, J., Martínez, S., Karatas, T., Bullo, F. 2004. Coverage control for mobile sensing networks, IEEE Transactions on Robotics and Automation 20(2), 243-255. DOI 10.1109/TRA.2004.824698
[11] Breitenmoser, A., Schwager, M., Metzger, J.-C., Siegwart, R., Rus, D. 2010. Voronoi coverage of non-convex environments with a group of networked robots, Proceedings of the IEEE International Conference on Robotics and Automation 4982- 4989. DOI 10.1109/ROBOT.2010.5509696
[12] Lee, S.G., Diaz-Mercado, Y., Egerstedt, M. 2015. Multirobot control using time-varying density functions, IEEE Transactions on Robotics 31(2) 489-493, DOI 10.1109/TRO.2015.2397771
[13] Bhattacharya, P., Gavrilova, M. L. 2007. Voronoi diagram in optimal path planning, 4th International Symposium on Voronoi Diagrams in Science and Engineering (ISVD 2007) 38-47. DOI 10.1109/ISVD.2007.43
[14] Sun, W., Dou, L., Chen, J., Fang, H. 2010. A multi-robot target tracking algorithm with centroidal Voronoi tessellation and consensus strategy, Proceedings of the 29th Chinese Control Conference, Beijing, 4607-4612
[15] Barnett, J. 2018. Prismatic axis, differential-drive robotic kiwifruit harvester for reduced cycle time, Master of Engineering Thesis
[16] Hiwin, https://www.hiwin.com/articulated-robots.html (accessed 8 June 2019).